CSIRO PUBLISHING

Reproduction, Fertility and Development
http://dx.doi.org/10.1071/RD14166

Transcriptome of early embryonic invasion at implantation sites in a murine model

J. M. Moreno-Moya[A,*], *N. A. Franchi*[B,E,*], *S. Martínez-Escribano*[A], *J. A. Martínez-Conejero*[A], *S. Bocca*[B], *S. Oehninger*[B,†] *and J. A. Horcajadas*[C,D,F,†]

[A]Fundación IVI (FIVI)–Instituto Universitario IVI (IUIVI), University of Valencia, Parc Científic Universitat de València, Catedrático Agustín Escardino, 9, 46980 – Paterna, Valencia, Spain.
[B]The Jones Institute for Reproductive Medicine, Department of Obstetrics and Gynecology, Eastern Virginia Medical School, Norfolk, VA 23507, USA.
[C]Araid at I+CS and Unviersidad Pablo de Olavide, Sevilla, Hospital Miguel Servet, Zaragoza, Spain.
[D]Universidad Pablo de Olavide, Sevilla, Spain.
[E]Present address: Instituto de Investigaciones Biológicas y Tecnológicas (IIBYT), CONICET and Facultad de Ciencias Exactas, Físicas y Naturales, Universidad Nacional de Córdoba, Argentina.
[F]Corresponding author. Email: jose.horcajadas@gmail.com

Abstract. Successful implantation relies on the interaction between a competent embryo and a receptive endometrium. The aim of the present study was to investigate genes differentially expressed in early invasive embryonic tissue versus decidual tissue in mice. Samples were obtained from the ectoplacental cone, the immediately surrounding deciduas and from deciduas from interimplantation sites. Microarray analysis showed that 817 genes were differentially expressed between extra-embryonic tissue and the surrounding decidua and that 360 genes were differentially expressed between the different deciduas, with a high representation of developmental processes. Genes differentially expressed in the maternal compartment included chemokines, lipoproteins, growth factors and transcription factors, whereas the embryonic invasive tissue expressed genes commonly observed in invasive tumour-like processes. These results provide information about genes involved in early embryonic invasion and the control exerted by the surrounding decidua. This information may be useful to find targets involved in pathologies associated with implantation failure and early pregnancy loss.

Additional keywords: ectoplacental cone, decidual tissue, microarray, mouse implantation, RNA expression patterns, trophoblast invasion.

Received 20 May 2014, accepted 23 January 2015, published online 5 May 2015

Introduction

The embryo implantation process is one of the mysteries of reproductive biology. Many aspects regarding the molecular basis of endometrial receptivity and the reciprocal interactions taking place between the blastocyst and endometrium remain unknown (Hou *et al.* 2004; Yoshinaga 2008). It was only in the past decade that similarities between the behaviour of placental cells and invasive cancer cells became apparent. However, although embryonic invasion is both temporally and locally controlled, tumour progression and metastasis are uncontrolled and occur with neither help nor restraint of the host tissue invaded by the tumour (Ferretti *et al.* 2007; Moreno 2008). Defective placentation is thought to be responsible for some diseases of pregnancy, such as pre-eclampsia. The pathology of this disease includes fewer trophoblasts, and their failure to invade the endometrium sufficiently with under-development of spiral arteries (Meekins *et al.* 1994; Zhou *et al.* 1997). However, the underlying molecular defects of the disease remain to be determined.

The window of implantation in humans appears to be restricted to Days 20–24 of the cycle (Davies *et al.* 1990). Human endometrial tissue has been widely analysed during these cycle days from the point of view of functional genomics (Horcajadas *et al.* 2007). Uterine epithelial cells of the decidualised endometrium secrete growth factors, cytokines and other molecules that act on the conceptus to ensure that its development is in concert with the uterus. Initially, the blastocyst interacts with the decidualised endometrial surface by apposition and attachment. The

*These authors contributed equally to this work.
†These authors contributed equally to this work.

invasive phase involves attachment of the invading trophoblast to the extracellular matrix (ECM), degradation of the matrix, migration and eventually replacement of the decidual artery endothelium with a new trophoblast phenotype, the vascular trophoblast cells (Cross *et al.* 1994). The establishment of an angiogenic phenotype leading to formation of new blood vessels, eventually resulting in vascular adaptation, is a key event in mammalian implantation (Smith 2000), the vasculogenesis process being essential to placental growth and successful development of the fetus. Production of matrix metalloproteinases (MMPs) by the invading trophoblast and tissue inhibitors of metalloproteinases (TIMPs) by the surrounding stromal cells (Fluhr *et al.* 2008) are of paramount importance for tissue reorganisation during trophoblast invasion. In addition, acquisition of a different immunological profile consisting of various subtypes of leucocytes (including T cells, macrophages and large granular lymphocytes) and the secretion of immunomodulatory factors are likely to play a fundamental role in implantation (Tulppala *et al.* 1995; Johnson *et al.* 1999; Lobo *et al.* 2004; Jabbour *et al.* 2006; Lea and Sandra 2007).

Although there are spatial and temporal differences between mouse and human implantation, studies using the mouse model have provided insights into the molecular basis of human implantation because of the existence of some important shared features. In both species, implantation leads to stromal decidualisation and the placentation is haemochorial. Conversely, several studies were based on models that do not reflect the natural process (Chen *et al.* 2006; Popovici *et al.* 2006; Marchand *et al.* 2011), most of them using *in vitro* systems (Popovici *et al.* 2006; Marchand *et al.* 2011; Giritharan *et al.* 2012), which are far from physiological conditions.

The purpose of the present study was to assess uterine and embryonic gene expression during the early invasive phase of placentation in the murine model, paying particular attention to the origin of tissue, which has not been adequately taken into account in earlier studies. Microarray analysis was used to determine RNA expression patterns for the early extra-embryonic tissue (ET) coming from the ectoplacental cone and for two different types of decidual tissues, namely the surrounding decidua (SD) covering the implanted embryo and decidual tissue located at interimplantation sites (ID).

Materials and methods

Tissue collection

All procedures involving mice were conducted in accordance with the Guide for the Care and Use of Laboratory Animals of the National Institutes of Health (NIH; http://grants.nih.gov/grants/olaw/Guide-for-the-care-and-use-of-laboratory-animals.pdf, accessed January 2011). The study design and experimental protocols were approved by the Institutional Animal Care and Use Committee at the University of Valencia. Adult and sexually mature (6–8-week-old B6CBA F1/J) virgin female mice were mated with CD1 fertile males. The following morning was considered Day 0 of pregnancy if the vaginal plug was observed. Mice were killed by cervical dislocation 6.5 days post-coitum (d.p.c.; $n = 3$ mice). Uterine segments were divided into implantation and interimplantation tissues by sharp dissection, as described previously (Shea and Geijsen 2007). Regarding the embryo, only the ectoplacental cone formed by the invasive trophoblast cells was studied and the deciduas were dissected free from the two types of implantation tissues. All tissues were immediately subjected to RNA extraction.

RNA isolation and microarray hybridisation

Total RNA was isolated from each tissue type and subjected to microarray analyses as described previously (Horcajadas *et al.* 2008). Briefly, total RNA was extracted using Trizol reagent (Life Technologies, Paisley, UK) and treated with DNase I (Promega, Southampton, UK) for 30 min at 37°C and then re-extracted with Trizol. RNA quality was assessed with an A2100 bioanalyzer (Agilent Technologies, Santa Clara, CA, USA). Only those samples with an RNA integrity number (RIN) >7.5 were included for microarray analysis. Then, 1 μg of each RNA sample was labelled with Cy3 according to manufacturer recommendations and hybridised to the One-Colour Agilent Whole Mouse Genome Microarray 44K (Agilent Technologies). Each tissue type was analysed in triplicate for each mouse.

Data processing and analysis

Spot intensities (median values) without background subtraction were $\log_2$ transformed to stretch data without changing the relationship between values. Data were normalised by quantile normalisation to compensate for systematic technical differences between chips, so as to see more clearly the systematic biological differences between samples. The replicates by gene symbol were merged by mean to obtain single gene intensity values and the data were filtered in order to delete unknown sequences or probes without gene description. R statistical software was used for these purposes and for downstream analysis (The R Development Core Team 2004).

The resulting matrix containing the previously mentioned log-transformed, normalised and merged-by-probe data was introduced into the paired Rank-Products module in MeV software (http://www.tm4.org/mev/) for statistical analysis. This method ranks genes according to their differential expression within each replicate and estimates the product of the ranks across them. Then, comparisons were made between the observed rank products and their sampling distribution under the null hypothesis to calculate whether they were identically distributed within each of the independent experiments. Samples were assigned to ET, SD or ID groups and then compared. A false discovery rate (FDR) correction of <5% was used and mRNA fold changes between the different samples and groups were calculated.

Gene ontology and ingenuity pathway analysis

The Database for Annotation Visualisation and Integrated Discovery (DAVID) was used for functional classification of an extensive list of genes (Dennis *et al.* 2003). Grouping genes on the basis of functional similarity can systematically enhance biological interpretation of large lists of genes derived from high-throughput studies. The functional classification tool generates a gene-to-gene similarity matrix based on shared functional annotation using over 75 000 gene ontology (GO) terms from 14 functional annotation sources.

Ingenuity pathway analysis (IPA) software (Ingenuity Systems, http://www.ingenuity.com/products/ipa) was used to find functions and most representative pathways. This tool uses the list of genes and their fold changes to find processes and functions significantly affected. The same software was used to generate gene product networks. This software uses its own 'ingenuity knowledge base', a repository of expertly curated biological interactions and functional annotations created from millions of individually modelled relationships between proteins, genes, complexes, cells, tissues, drugs and diseases. The curated content in the knowledge base is organised into an ontology that allows for contextual information, computation by the applications and synonym resolution to ensure consistency among concepts.

Hierarchical clustering and principal component analysis

Principal component analysis (PCA) was performed using the MeV 4.2.02 software (http://www.tm4.org/mev/). PCA was run to reduce the number of variables to principal components, which represents the majority of the variability in the dataset. A two-dimensional scatter plot was produced in order to visualise the differences in sample sets based on each sample's gene expression profile.

Quantitative reverse transcription–polymerase chain reaction validation of microarray data

cDNA was generated using the Advantage RT-for-PCR kit (Clontech, Palo Alto, CA, USA). Quantitative reverse transcription–polymerase chain reaction (qRT-PCR) was performed in triplicate using SYBR Green PCR Master Mix and a LightCycler instrument (Roche Diagnostics, Mannheim, Germany) according to the manufacturer's instructions. Relative quantification was performed by the standard curve method ($R^2 > 0.98$) taking into account the efficiency of the reaction (slope values between −3.1 and −3.4). Table 1 lists gene names, sequences of forward and reverse primers and expected PCR product sizes.

Results

Microarray data analysis

The source of the different tissues subjected to microarray analysis is shown in the experimental design represented schematically in Fig. 1*a*. As expected, the number of differentially expressed genes found when comparing ET with SD was higher than that detected when comparing SD with ID. The analysis contrasting the ectoplacental cone of ET with SD generated a list of 817 genes that were differentially expressed (fold change >2.0, $P < 0.05$); of these, 395 were overexpressed and 422 were underexpressed (see Table S1 available as Supplementary Material to this paper). The comparison between ID and SD produced a list of 360 differentially expressed genes (fold change >2.0, $P < 0.05$); of these, 237 were overexpressed and 123 were underexpressed (Table S2).

For all samples, a clustering analysis was performed using genes from the lists with $P < 0.05$. The PCA plot (Fig. 2*a*) illustrates the principal components of the nine samples from the three different tissues. Different individual samples from the same tissue type are grouped together, and all tissue types are separated from each other.

As shown in the clustering shown in Fig. 2*b*, extra-embryonic and decidual tissue samples segregate into two main, clearly differentiated clustering branches. Both extra-embryonic and decidual tissue samples self-clustered together, except for one of the interimplantation site samples (ID1), which showed dissimilarity (also visible in the PCA plot; Fig. 2*a*). The two major branches containing similar patterns of gene expression intensity discriminate ET from decidual tissues. The sub-branches within decidual tissue exhibit gene patterns differentiating ID from SD, the latter being the tissue that shows a higher number of overexpressed genes, possibly in response to the presence of the implanting embryo.

The 25 most over- and underexpressed genes in both comparisons are listed in Table 2, where gene symbol and description, GenBank accession numbers and fold changes are also given. As outlined in the Venn diagram in Fig. 1*b*, 123 genes (51 over- and 72 underexpressed) are shared by both comparisons.

Table 1. Primers used for quantitative reverse transcription–polymerase chain reaction

Gapdh, glyceraldehyde-3-phosphate dehydrogenase; *Slc13a4*, solute carrier family 13 (sodium/sulfate symporters), member 4; *Bex4*, brain expressed gene 4; *Dio3*, deiodinase, iodothyronine type III; *Sfrp5*, secreted frizzled-related sequence protein 5; *Erv3*, endogenous retroviral sequence 3; *Cnn1*, calponin 1; *Pcp4*, Purkinje cell protein 41b5; *Klk1b5*, kallikrein 1-related peptidase b5

Gene	Primers		PCR product (bp)
	Forward (5′–3′)	Reverse (5′–3′)	
Gapdh	TGCTGAGTATGTCGTGGA	CAGGATGCATTGCTGACA	183
Slc13a4	CCCGGCTTTGTCCCTGGCTG	GGCGTAGCCTCCTCCCACCA	243
Bex4	TGCCCTCGCTCACTCTCTCC	AATTTGGATGCCATCACTCCTGGGC	228
Dio3	AGGCGAGGAGATGCCCCCTG	ATTGAGCACCAACGGGCGGG	226
Sfrp5	GCACAGCGCTGATGGCCCTCA	GGGCAGCTTGCCCGTTCTT	201
Erv3	GAGCCACCAGCCCTCAGCAC	GCAGTGGACCTCTGAAAGCAGCC	215
Cnn1	GGAGGCTCGGCTGCCTGTTG	AGTTGTTCCCGATGCGCCGG	219
Pcp4	GGAAGCAGCCACCCCTGAGC	AATGGCCACAGCTGCACGCT	207
Klk1b5	TGCGGGGGAGTCCTGCTGAA	GGCGGAGCAGCATCAGGTCA	229

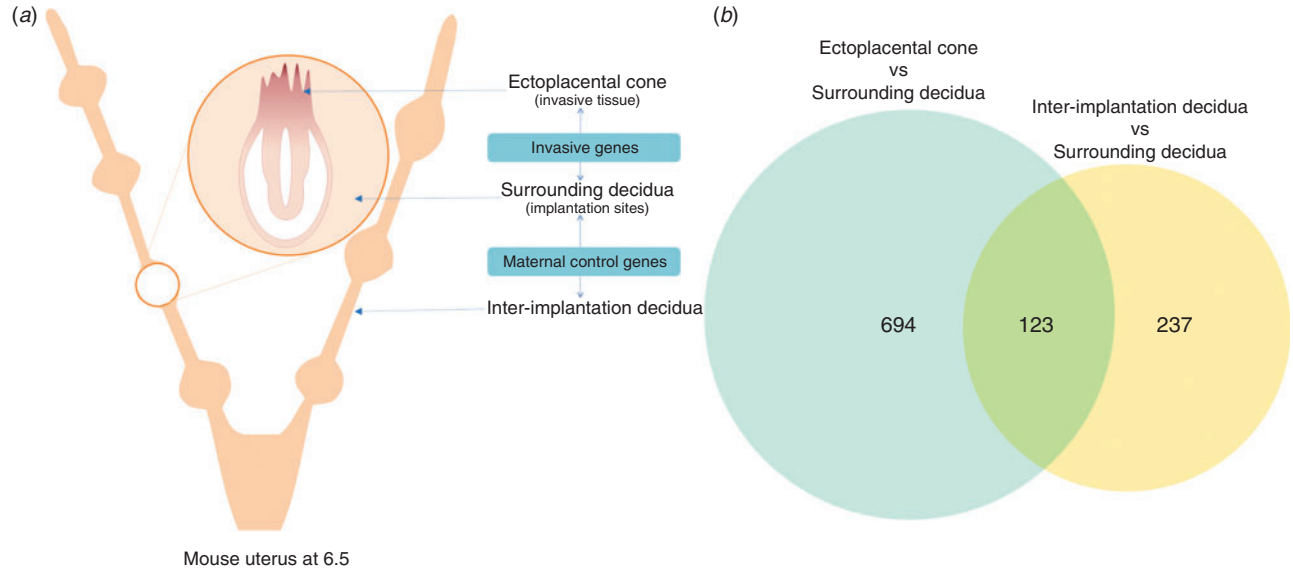

Fig. 1. (*a*) Diagram of the experimental design indicating the source of the different tissues analysed in the present study. (*b*) Venn diagram referring the number of differentially expressed genes in the two comparisons (extra-embryonic tissue versus surrounding decidua and interimplantation decidua versus surrounding decidua) and the 123 genes shared by both of them.

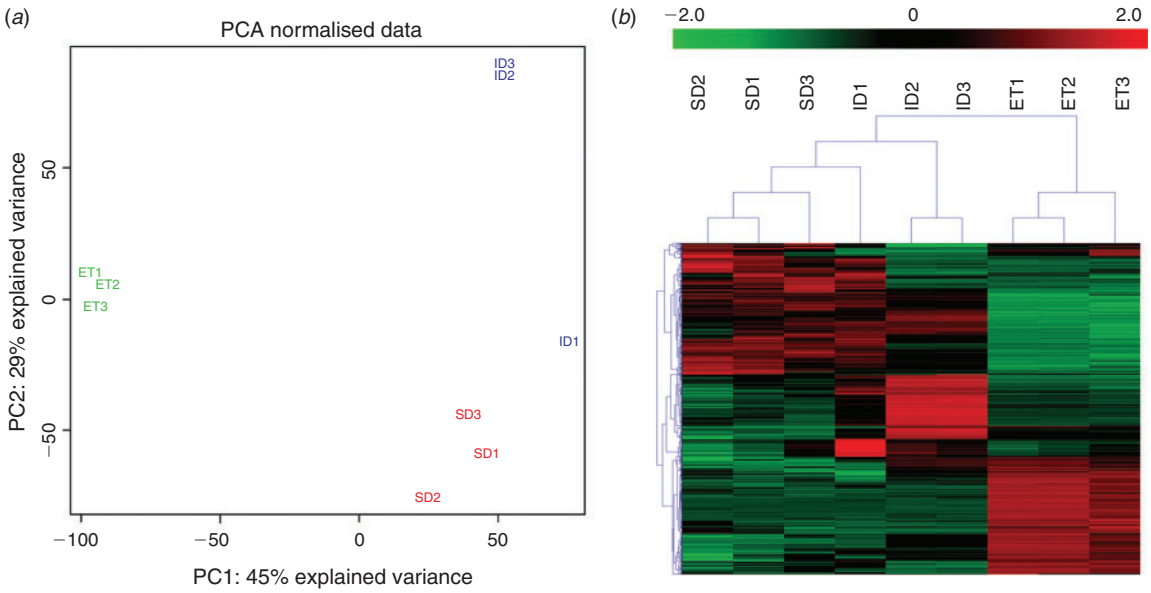

Fig. 2. Unsupervised clustering analysis of differentially expressed genes with *P*-values <0.05 in samples from extra-embryonic tissue (ET), surrounding decidua (SD) and interimplantation decidua (ID). (*a*) Principal component analysis (PCA) showing the principal components (PC) of nine samples from the three different tissues. Different individual samples from the same tissue type grouped together, and all tissue types are clearly separated from each other. (*b*) Dendrogram showing extra-embryonic and decidual tissues samples segregating into two major clustering branches that can be clearly differentiated. The sub-branches within decidual tissue exhibit gene patterns differentiating ID from SD.

qRT-PCR validation of microarray data

Primers sequences used for RT-PCR, as well as the expected size of PCR products, are listed in Table 1.

As shown in Fig. 3, mRNA expression levels were similar according to both microarray and qPCR for every gene analysed, thus validating microarray data. This was true both for ET versus SD and for ID versus SD (Fig. 3*a*, *b*). In ET tissue, type 3 iodothyronine deiodinase (*Dio3*), secreted frizzled-related protein 5 (*Sfrp5*) and endogenous retroviral sequence 3 (*Erv3*) mRNA expression was lower than in SD (43-fold for *Dio3*, and

Table 2. First 25 over- and 25 underexpressed genes in extra-embryonic tissue (ET) versus surrounding decidua (SD) and interimplantation decidua (ID) vs SD

Gene symbol	Fold change	GenBank accession no.	Description
ET versus SD			
Overexpressed			
Apoc2	321.25	NM_009695	*Mus musculus* apolipoprotein C-II
Slc13a4	235.73	NM_172892	*Mus musculus* solute carrier family 13 (sodium/sulfate symporters), member 4
Bex4	161.42	NM_212457	*Mus musculus* brain expressed gene 4
Bex1	134.20	NM_009052	*Mus musculus* brain expressed gene 1
Hbb-bh1	131.56	NM_008219	*Mus musculus* haemoglobin Z, beta-like embryonic chain
Afp	128.98	NM_007423	*Mus musculus* alpha fetoprotein
Apom	117.01	NM_018816	*Mus musculus* apolipoprotein M
Amn	112.05	NM_033603	*Mus musculus* amnionless
Ascl2	97.00	NM_008554	*Mus musculus* achaete-scute complex homologue 2 (*Drosophila*)
Tdh	82.58	NM_021480	*Mus musculus* L-threonine dehydrogenase
Clic6	75.32	NM_172469	*Mus musculus* chloride intracellular channel 6
Hnf4a	69.91	NM_008261	*Mus musculus* hepatic nuclear factor 4, alpha
Ttr	66.35	NM_013697	*Mus musculus* transthyretin
Cubn	65.45	NM_001081084	*Mus musculus* cubilin (intrinsic factor-cobalamin receptor)
Cited1	64.19	NM_007709	*Mus musculus* Cbp/p300-interacting transactivator with Glu/Asp-rich carboxy-terminal domain 1
Cdx1	63.04	NM_009880	*Mus musculus* caudal type homeobox 1
Bex2	60.22	NM_009749	*Mus musculus* brain expressed X-linked 2
Apoa1	60.12	NM_009692	*Mus musculus* apolipoprotein A-I
Aldob	57.13	NM_144903	*Mus musculus* aldolase B, fructose-bisphosphate
Lrp2	55.43	NM_001081088	*Mus musculus* low-density lipoprotein receptor-related protein 2
Gldc	54.14	NM_138595	*Mus musculus* glycine decarboxylase (Gldc)
Lgals2	53.72	NM_025622	*Mus musculus* lectin, galactose-binding, soluble 2
Cdx2	48.14	NM_007673	*Mus musculus* caudal type homeobox 2
Soat2	44.76	NM_146064	*Mus musculus* sterol *O*-acyltransferase 2
Phlda2	41.31	NM_009434	*Mus musculus* pleckstrin homology-like domain, family A, member 2
Underexpressed			
Mgp	−101.10	NM_008597	*Mus musculus* matrix Gla protein
Dio3	−70.84	NM_172119	*Mus musculus* deiodinase, iodothyronine type III
Sfrp5	−68.79	NM_018780	*Mus musculus* secreted frizzled-related sequence protein 5
Mfap5	−68.01	NM_015776	*Mus musculus* microfibrillar associated protein 5
Cxcl14	−66.41	NM_019568	*Mus musculus* chemokine (C-X-C motif) ligand 14
Trem2	−44.76	NM_031254	*Mus musculus* triggering receptor expressed on myeloid cells 2
Ly6a	−43.80	NM_010738	*Mus musculus* lymphocyte antigen 6 complex, locus A
Tac2	−42.78	NM_009312	*Mus musculus* tachykinin 2
Gpr115	−42.50	NM_030067	*Mus musculus* G-protein-coupled receptor 115
Ano1	−42.31	NM_178642	*Mus musculus* anoctamin 1, calcium-activated chloride channel
Erv3	−42.29	NM_001166206	*Mus musculus* endogenous retroviral sequence 3
Wnt10a	−42.24	NM_009518	*Mus musculus* wingless related MMTV integration site 10a
A2m	−42.08	NM_175628	*Mus musculus* alpha-2-macroglobulin
Sfrp4	−41.84	NM_016687	*Mus musculus* secreted frizzled-related protein 4
Lbp	−38.16	NM_008489	*Mus musculus* lipopolysaccharide-binding protein
Dmkn	−37.94	NM_001166173	*Mus musculus* dermokine (Dmkn), transcript variant 3
Aqp1	−37.65	NM_007472	*Mus musculus* aquaporin 1
Gpihbp1	−37.09	NM_026730	*Mus musculus* GPI-anchored HDL-binding protein 1
Smoc2	−35.89	NM_022315	*Mus musculus* SPARC-related modular calcium binding 2
Kazald1	−35.80	NM_178929	*Mus musculus* Kazal-type serine peptidase inhibitor domain 1
Olfml3	−35.36	NM_133859	*Mus musculus* olfactomedin-like 3
Tm4sf1	−34.32	NM_008536	*Mus musculus* transmembrane 4 superfamily member 1
Alox5	−33.85	NM_009662	*Mus musculus* arachidonate 5-lipoxygenase
Dpep1	−33.78	NM_007876	*Mus musculus* dipeptidase 1 (renal)
Des	−33.72	NM_010043	*Mus musculus* desmin

(*Continued*)

Table 2. (Continued)

Gene symbol	Fold change	GenBank accession no.	Description
ID versus SD			
Overexpressed			
Cnn1	298.00	NM_009922	*Mus musculus* calponin 1
Pcp4	126.63	NM_008791	*Mus musculus* Purkinje cell protein 4
Klk1b5	124.67	NM_008456	*Mus musculus* kallikrein 1-related peptidase b5
Ccl21a	120.58	NM_011124	*Mus musculus* chemokine (C-C motif) ligand 21A
Egfbp2	97.66	NM_010115	*Mus musculus* epidermal growth factor binding protein type B
Napsa	97.47	NM_008437	*Mus musculus* napsin A aspartic peptidase
Guca2b	91.03	NM_008191	*Mus musculus* guanylate cyclase activator 2b (retina)
Actg2	80.26	NM_009610	*Mus musculus* actin, gamma 2, smooth muscle, enteric
Trpv6	75.43	NM_022413	*Mus musculus* transient receptor potential cation channel, subfamily V, member 6
Tmem213	71.98	NM_029921	*Mus musculus* transmembrane protein 213
Tmprss4	68.55	NM_145403	*Mus musculus* transmembrane protease, serine 4
Klk1	65.28	NM_010639	*Mus musculus* kallikrein 1
Hdc	52.33	NM_008230	*Mus musculus* histidine decarboxylase
Mfap4	52.17	NM_029568	*Mus musculus* microfibrillar-associated protein 4
Csf1	51.19	NM_007778	*Mus musculus* colony stimulating factor 1 (macrophage), transcript variant 1
Mmp7	50.29	NM_010810	*Mus musculus* matrix metallopeptidase 7
Serpina1e	49.31	NM_009247	*Mus musculus* serine (or cysteine) peptidase inhibitor, clade A, member 1E
Aqp5	46.88	NM_009701	*Mus musculus* aquaporin 5
Gabrp	46.21	NM_146017	*Mus musculus* gamma-aminobutyric acid (GABA) A receptor, pi
Sftpd	46.08	NM_009160	*Mus musculus* surfactant associated protein D
Wfdc2	44.89	NM_026323	*Mus musculus* WAP four-disulfide core domain 2
Cdh16	43.67	NM_007663	*Mus musculus* cadherin 16
Slc27a2	43.14	NM_011978	*Mus musculus* solute carrier family 27 (fatty acid transporter), member 2
Serpina1a	39.79	NM_009243	*Mus musculus* serine (or cysteine) peptidase inhibitor, clade A, member 1A
Prss28	39.63	NM_053259	*Mus musculus* protease, serine, 28
Underexpressed			
Prl3d2	−69.90	NM_172155	*Mus musculus* prolactin family 3, subfamily d, member 1
A2m	−59.11	NM_175628	*Mus musculus* alpha-2-macroglobulin
Sfrp5	−48.79	NM_018780	*Mus musculus* secreted frizzled-related sequence protein 5
Tdo2	−36.42	NM_019911	*Mus musculus* tryptophan 2,3-dioxygenase
Prl3d1	−35.66	NM_008864	*Mus musculus* prolactin family 3, subfamily d, member 1
Ceacam15	−30.07	NM_175315	*Mus musculus* carcinoembryonic antigen-related cell adhesion molecule 15
Plac1	−25.33	NM_019538	*Mus musculus* placental specific protein 1
Prl2c5	−25.29	NM_181852	*Mus musculus* prolactin family 2, subfamily c, member 5
Wnt10a	−24.48	NM_009518	*Mus musculus* wingless related MMTV integration site 10a
Cyp11a1	−24.35	NM_019779	*Mus musculus* cytochrome P450, family 11, subfamily a, polypeptide 1
Erv3	−23.49	NM_001166206	*Mus musculus* endogenous retroviral sequence 3
Gdpd2	−22.50	NM_023608	*Mus musculus* glycerophosphodiester phosphodiesterase domain containing 2
Prl7a1	−22.16	NM_001164058	*Mus musculus* prolactin family 7, subfamily a, member 1, transcript variant 1,
Prl8a9	−21.54	NM_023332	*Mus musculus* prolactin family8, subfamily a, member 9
Sct	−21.38	NM_011328	*Mus musculus* secretin
Gpr115	−20.59	NM_030067	*Mus musculus* G-protein-coupled receptor 115
Crct1	−20.30	NM_028798	*Mus musculus* cysteine-rich C-terminal 1
Krtdap	−18.09	NM_001033131	*Mus musculus* keratinocyte differentiation associated protein
Adm	−17.90	NM_009627	*Mus musculus* adrenomedullin
Atoh8	−17.77	NM_153778	*Mus musculus* atonal homologue 8 (*Drosophila*)
Slc6a12	−17.37	NM_133661	*Mus musculus* solute carrier family 6 (neurotransmitter transporter, betaine/GABA), m12
Nccrp1	−17.24	NM_001081115	*Mus musculus* non-specific cytotoxic cell receptor protein 1 homologue (zebrafish)
Dmkn	−16.93	NM_001166173	*Mus musculus* dermokine, transcript variant 3
Ass1	−16.92	NM_007494	*Mus musculus* argininosuccinate synthetase 1
Mt4	−16.56	NM_008631	*Mus musculus* metallothionein 4

74-fold for the other two genes). The overexpressed genes included solute carrier family 13 (sodium/sulfate symporters), member 4 (*Slc13a4*) and brain expressed gene 4 (*Bex4*) (390-fold increase in expression). Conversely, in ID tissue, *Dio3* expression was 11-fold lower than in SD and *Sfrp5* and *Erv3* expression was approximately 29-fold lower in ID. In addition, calponin 1 (*Cnn1*), Purkinje cell protein 4 (*Pcp4*), and kallikrein 1-related peptidase b5 (*Klk1b5*) mRNA expression was

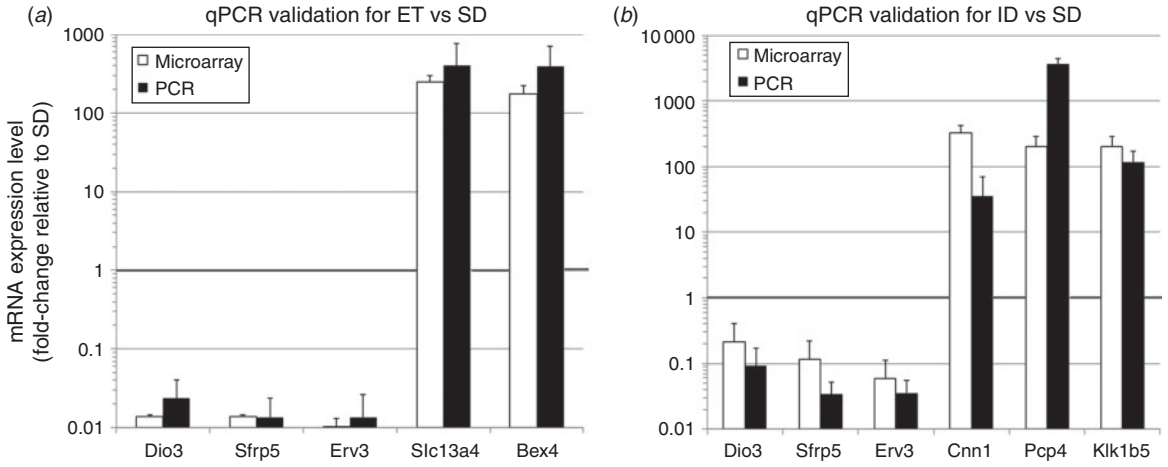

Fig. 3. Quantitative polymerase chain reaction (PCR) validation of microarray data. mRNA expression of genes analysed by microarray (□) was validated by quantitative reverse transcription–polymerase chain reaction (■) for comparisons of (*a*) extra-embryonic tissue (ET) versus surrounding decidua (SD) and (*b*) interimplantation decidua (ID) versus SD. Data show mean (± s.e.m.) values for each gene normalised against the mean value of the housekeeping gene *Gapdh*, and are expressed as fold changes of gene expression in SD tissue. n = three mice.

Table 3. Gene ontology terms over-represented in extra-embryonic tissue (ET) versus surrounding decidua (SD) and interimplantation decidua (ID) vs SD

FDR, false discovery rate

Gene ontology term	FDR
ET versus SD	
Developmental process	9.50×10^{-17}
System development	1.60×10^{-15}
Multicellular organismal development	9.60×10^{-15}
Anatomical structure development	1.10×10^{-14}
Organ development	7.40×10^{-14}
Tissue development	2.90×10^{-8}
Positive regulation of biological process	2.10×10^{-6}
Embryonic development	4.30×10^{-6}
Cell differentiation	1.00×10^{-5}
Tube development	1.30×10^{-5}
Positive regulation of cellular process	6.90×10^{-5}
Cellular developmental process	1.10×10^{-4}
Anatomical structure morphogenesis	1.40×10^{-4}
Lipid localization	3.90×10^{-4}
Lipid transport	5.10×10^{-4}
Heart development	1.30×10^{-3}
In utero embryonic development	1.90×10^{-3}
Embryonic development ending in birth or egg hatch	2.10×10^{-3}
Chordate embryonic development	4.00×10^{-3}
Respiratory system development	4.30×10^{-3}
Regulation of cell proliferation	6.60×10^{-3}
Skeletal system development	7.60×10^{-3}
Response to external stimulus	8.70×10^{-3}
Enzyme-linked receptor protein signalling pathway	8.90×10^{-3}
Regulation of developmental process	1.30×10^{-2}
Respiratory tube development	1.90×10^{-2}
Negative regulation of biological process	2.00×10^{-2}
Acute inflammatory response	2.20×10^{-2}
Anterior/posterior pattern formation	2.80×10^{-2}
Organ morphogenesis	4.40×10^{-2}
Tube morphogenesis	4.50×10^{-2}
ET versus SD	
Response to external stimulus	4.90×10^{-3}
Response to wounding	2.70×10^{-2}
Response to chemical stimulus	4.00×10^{-2}

(*Continued*)

Table 3. (Continued)

upregulated (35-, 3650- and 116-fold, respectively) compared with SD tissue.

GO analysis and IPA of differentially expressed genes

Differentially expressed genes were subjected to GO analysis to identify biological terms statistically over-represented. Table 3 summarises the over-represented terms in both analyses and the FDR, which indicates the statistical significance, for all genes (FDR <0.05). Most genes in the comparison of ET with SD belong to biological terms related to development, organ and embryonic development, morphogenesis and cell proliferation and differentiation. In the comparison of ID with SD, the genes analysed were related to responses to wounding and external stimuli.

Differentially expressed genes were also analysed by IPA software to find over-represented biological functions, canonical pathways and gene networks. For the 817 differentially expressed genes in the ET versus SD comparison, pathways related to tissue, organ and embryonic development were the most represented terms (Fig. 4*a*), whereas in the case of ID versus SD, 'immune cell trafficking' was one of the most represented processes (Fig. 4*b*), which was not observed through GO analysis.

Canonical pathways found for the analysis of ET versus SD were primarily related to *Oct4* and *Nanog*, which are critical for

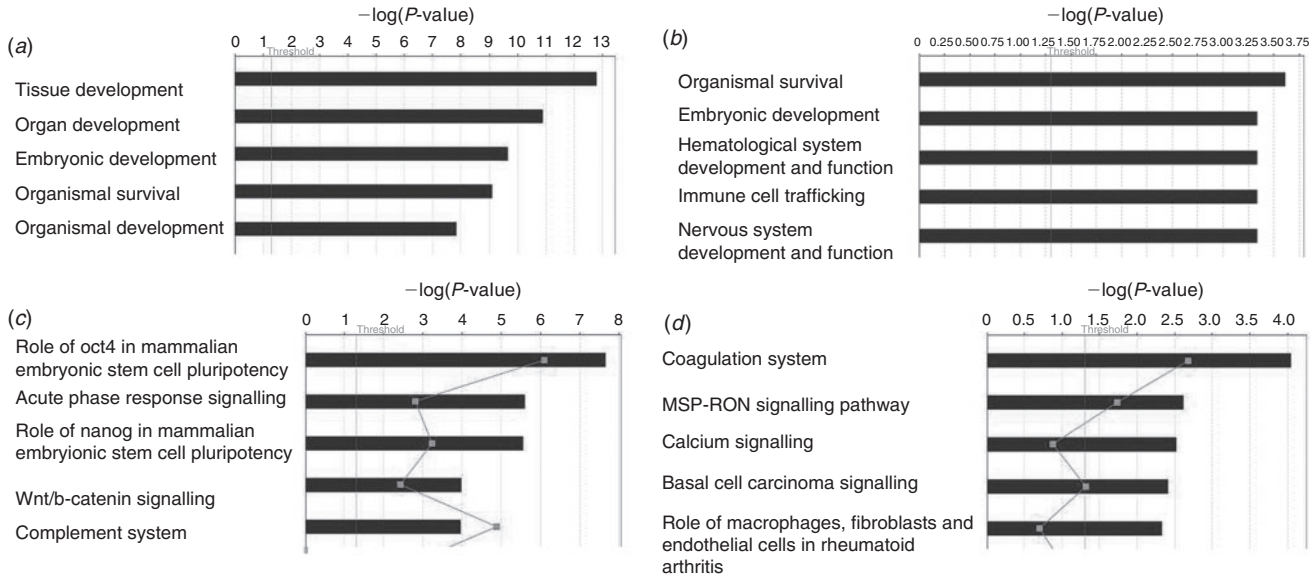

Fig. 4. Ingenuity pathway analysis. Results show physiological system development and function analysis for (*a*) extra-embryonic tissue (ET) versus surrounding decidua (SD) and (*b*) interimplantation decidua (ID) versus SD, and canonical pathways over-represented for (*c*) ET versus SD and (*d*) ID versus SD.

self-renewal of undifferentiated embryonic stem cells (Fig. 4*c*). The Wnt/β-catenin signalling pathway, involved in normal patterning of embryo development, was highly represented. In the case of ID versus SD, canonical pathways with the highest representation were associated with the coagulation system, macrophage stimulation, calcium signalling and carcinoma (Fig. 4*d*).

IPA revealed several interaction networks associated with differentially expressed genes. In the analysis of ET versus SD, the first interaction network contained genes involved in cell cycle, cellular movement, growth and proliferation (Fig. 5*a*), whereas the second highest network showed several genes connected with inflammatory responses (Fig. 5*b*). In the analysis of ID versus SD, the most important network was implicated in cell movement and immune cell trafficking (Fig. 6*a*) and the second network was involved in DNA replication, recombination and repair, cell death and cellular development (Fig. 6*b*).

Discussion

The nature of embryonic signals influencing uterine functions is mostly unknown. In rodents and humans, the limiting factor to address this question is the availability of adequate amounts of tissue for analysis, although with the advent of genomics it is now possible to identify embryonic signals during implantation. Several transcriptomics studies have been conducted with the purpose of finding the maternal role in early embryo implantation, but these studies had several limitations. Some used models that deviate from the natural or physiological situation (Chen *et al.* 2006; Popovici *et al.* 2006; Marchand *et al.* 2011); most investigated only one of the tissues, either the endometrium or the embryo and others examined the interaction between embryonic and maternal tissue using *in vitro* models (Popovici *et al.* 2006; Marchand *et al.* 2011; Giritharan *et al.* 2012). Although such publications represent the only possible approach to human implantation studies, they do not reflect the complexity of the natural process. In fact, recently published results have shown a reduced differential gene expression between the inner cell mass and trophectoderm in mouse embryos derived from *in vitro* cultures compared with those obtained *in vivo* (Giritharan *et al.* 2010). In the present study, we examined the early murine pregnancy, when the embryo is invading the uterine endometrium, giving special importance to the origin of the tissues to be analysed. To the best of our knowledge, this is the first study in which microarray analysis has been used to describe gene expression by the early invading embryonic and adjacent maternal tissues.

The microarrays were performed on ET, SD and ID tissues. Two parallel analysis were accomplished: the first was a comparison between ET and SD that resulted in a list of differentially expressed genes involved in invasion (hereafter referred to as ‘invasive genes’), whereas the second compared ID with SD and generated a list of differentially expressed genes involved in maternal adaptation to the embryo (hereafter referred to as ‘maternal control genes’; Fig. 1*a*).

The microarray analysis between ET and SD generated an extensive list of invasive genes (Table 2). Some of the most overexpressed genes in the ET, such as apolipoprotein C-II (*Apoc2*) and solute carrier family 13 (sodium/sulfate symporters), member 4 (*Slc13a4*), have been described previously as highly expressed in extra-embryonic tissue (Dawson *et al.* 2005; Ishida *et al.* 2007). Specifically, *Slc13a4* expression has been localised to cell clusters at the leading edge of the chorion in mouse placentas and plays a role in mediating sulfate supply to the fetus (Dawson *et al.* 2012), with the loss of placental *Slc13a4* being embryonic lethal (Rakoczy *et al.* 2014). Our results confirm the abundant expression of *Slc13a4* by the invading embryonic tissue and therefore its importance in the development of the maternal–fetal interface.

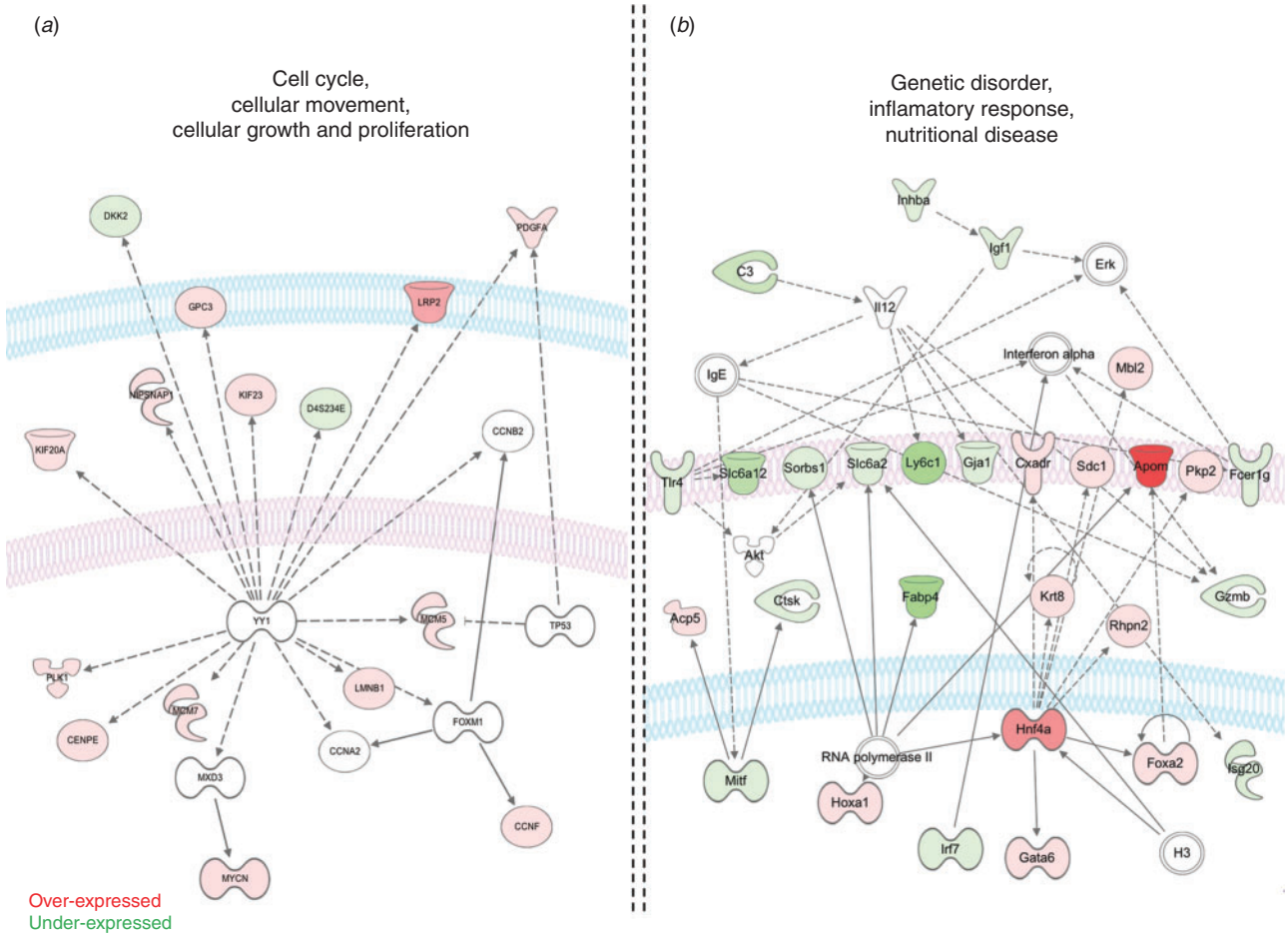

Fig. 5. Ingenuity pathway analysis (IPA) showing interaction networks for extra-embryonic tissue (ET) versus surrounding decidua (SD). The network displays nodes (genes/gene products) and edges (the biological relationship between nodes). The intensity of the node colour indicates the degree of overexpression (red) or underexpression (green) associated with a particular gene in extra-embryonic tissue (ET) compared with SD. Different shapes in the nodes represent functional classes of the gene product. Solid and dashed lines represent direct and indirect interactions, respectively. (*a*) IPA network analysis 1. Differentially expressed genes in ET versus SD are involved in cell cycle, cell movement, cell growth and proliferation. (*b*) IPA network analysis 2. Differentially expressed genes in ET versus SD are primarily involved in inflammatory responses.

Moreover, some of the genes highly overexpressed in SD, such as secreted frizzled-related protein 5 (*Sfrp5*) and chemokine (C-X-C motif) ligand 14 (*Cxcl14*), are involved in tumour growth restriction (Takagi *et al.* 2008) and control of trophoblast invasion (Kuang *et al.* 2009), respectively. In addition, *Cxcl14* was reported to be downregulated in progressive endometrial cancer (van der Horst *et al.* 2012) and as a negative regulator of growth and metastasis in breast cancer (Gu *et al.* 2012), suggesting that *Cxcl14* has the role of negatively regulating invasion of the trophoblast into the uterine endometrium. MMPs and TIMPs are key molecules known to be involved in the invasion mechanisms used by both the embryo and tumour cells. In particular, a pronounced increase in *Mmp9* secretion by trophoblastic cells stimulated by human chorionic gonadotrophin (*in vitro*) has been reported (Fluhr *et al.* 2008), as well as the cooperation of *Mmp9* in promoting the *in vivo* invasive and angiogenic phenotype of malignant cells (Masson *et al.* 2005). Of the overexpressed genes reported in the present study, *Mmp9* and *Mmp23* are overexpressed in extra-embryonic tissue and *Timp1* and *Timp2* are overexpressed in the surrounding decidua (Table S1). These genes exemplify the importance of maternal control over the invading embryo.

Conversely, microarray analysis of ID and SD revealed 360 differentially expressed genes, such as cytokines and chemokines, which are involved in the migration and maturation of immune cells (Britschgi *et al.* 2010), and genes associated with inflammatory responses and organisation of the ECM (Hochepied *et al.* 2000), such as alpha-2-macroglobulin (*A2m*) (Table 2), which suggests that these genes are involved in the adaptation of the maternal environment to the embryo. The most represented GO terms in the analysis of ET versus SD are all involved in development (Table 3), similar to the results obtained using IPA software (‘Physiological System Development and Function’; Fig. 4*a*). The Wnt/β-catenin signalling pathway is highly represented in the ET versus SD (Fig. 4*c*), and appears to be involved in the maternal response to embryo

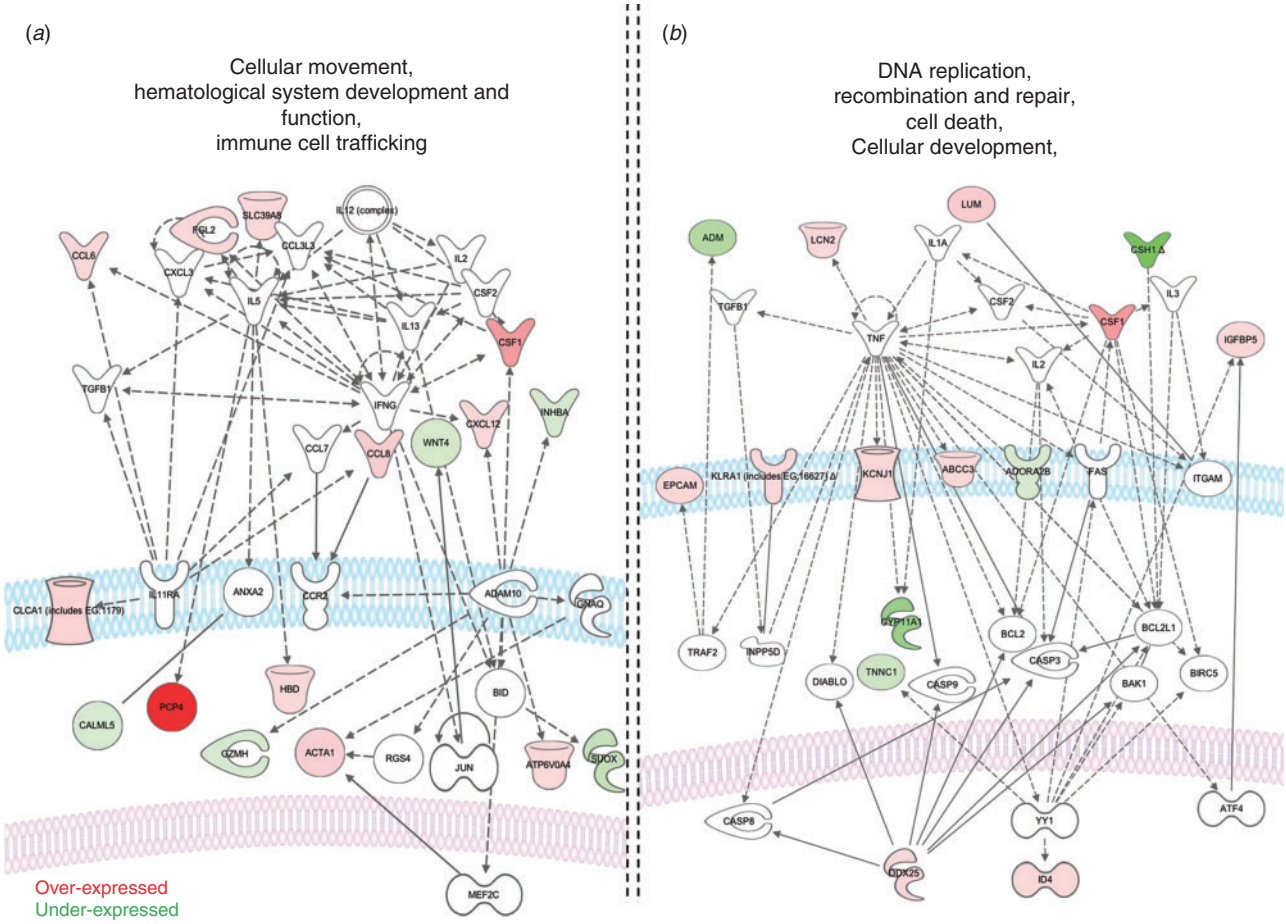

Fig. 6. Ingenuity pathway analysis (IPA) showing interaction networks for interimplantation decidua (ID) versus surrounding decidua (SD). (*a*) IPA network analysis 1. Differentially expressed genes in ID versus SD are involved in cellular movement, haematological system development and function, and immune cell trafficking. (*b*) IPA network analysis 2. Differentially expressed genes in ID versus SD involved in DNA replication, recombination and repair, cell death and cellular development.

invasion, as described recently (Franco *et al.* 2011). From the analysis of ID versus SD using DAVID, the GO terms most represented were those involved in response to a stimulus, which is consistent with the idea that embryo implantation generates an important stimulus in the mother (Table 3). The results of the IPA software for 'Physiological System Development and Function' and 'Canonical Pathways' over-represented in the case of ID versus SD, highlights 'immune traffic' as one of the important processes (Fig. 4*b*, *d*), which is consistent with the immune remodelling that the maternal uterus undergoes to support the developing embryo (Hess *et al.* 2007).

The main network shows several genes associated with cell cycle and cellular movement, growth and proliferation (Fig. 5*a*). Most of these genes were overexpressed by the ET, which is consistent with their rapid growth and proliferation. It is also notable that Yy1 transcription factor (*Yy1*) is a transcription factor that did not appear on the list of differentially expressed genes that centralises the main network. The second network of genes differentially expressed by the ET and SD has been shown to be involved in inflammatory processes (Fig. 5*b*). There is a greater representation of under-expressed genes, some of which are overexpressed in the SD, supporting the idea that inflammatory processes occur in the maternal tissue in response to embryo implantation.

The first network shown for the analysis of ID versus SD is related to cellular movement and immune cell trafficking (Fig. 6*a*). Among the genes of this network, *Wnt4* is one of the most important because it mediates progesterone-induced stromal decidualisation in mice and humans (Li *et al.* 2007) and is a critical regulator of embryo implantation (Franco *et al.* 2011). Interestingly, secreted frizzled-related protein 5 (*Sfrp5*), which is overexpressed in SD, is involved in inhibition of tumourigenesis by interfering with the Wnt pathway (Su *et al.* 2010; Stuckenholz *et al.* 2013).

Several genes from this network belong to the family of cytokines and chemokines, such as chemokine (C-C motif) ligand 8 (*Ccl8*), which is regulated in decidualised endometrial stromal fibroblasts in response to trophoblast-conditioned medium (Hess *et al.* 2007), and chemokine (C-X-C motif) ligand 12 (*Cxcl12*), which participates in the chemokine (C-X-C motif)

ligand 12–chemokine (C-X-C motif) receptor 4 (*Cxcl12–Cxcr4*) axis in the cooperation between trophoblast and decidual cells during human pregnancy, as recently reported by Ren *et al.* (2012). Another interesting gene network resulting from the analysis of ID versus SD is the one involved in DNA replication, recombination and repair, cell death and cellular development, processes all associated with uterine tissue remodelling in response to the presence of the implanting embryo (Fig. 6*b*).

In summary, the present study is the first to define the transcriptome of the early embryo implantation facing the issue from a new perspective, as it takes into consideration both the embryonic and the maternal sides during the *in vivo* process. The differentially expressed genes belonging to the 'invasive genes' group as well as 'maternal control genes' represent known and novel early markers of a successful invasive phase of the implantation process. The data presented herein are validated by the identification of genes previously implicated in cell invasion and invasion restriction, and bring into focus new players in the complex process of embryo invasion into the uterus. Genes identified in this study that are associated with embryo implantation and early maternal control at the implantation interface provide further insights into idiopathic reproductive diseases, such as recurrent implantation failure, pre-eclampsia and early pregnancy loss. At the same time, several of these genes support the hypothesis that cellular mechanisms used by placental cells during implantation are similar to those used by cancer cells to invade and spread within the body (Murray and Lessey 1999). Appreciation of the maternal mechanisms that control this invasive behaviour may lead to a better understanding of metastatic cancer cells and consequently to the development of better methods to control their growth and spread within host tissues. Finally, the identification of molecules involved in the invasive process of implantation could provide novel targets for the diagnosis and treatment not only of pathological pregnancies, but also cancers, enabling the translation, in the future, of basic research discoveries into effective clinical applications.

Acknowledgements

The authors would thank the Ministerio de Ciencia e Innovación of the Spanish Government (SAF2008-04349), and the Jones Institute Foundation (Norfolk, VA, USA) for financial support. The authors gratefully acknowledge Dr R. James Swanson (Old Dominion University, Norfolk, VA, USA) for his valuable help with the design of the experiments.

References

Britschgi, M. R., Favre, S., and Luther, S. A. (2010). CCL21 is sufficient to mediate DC migration, maturation and function in the absence of CCL19. *Eur. J. Immunol.* **40**, 1266–1271. doi:10.1002/EJI.200939921

Chen, Y., Ni, H., Ma, X. H., Hu, S. J., Luan, L. M., Ren, G., Zhao, Y. C., Li, S. J., Diao, H. L., Xu, X., Zhao, Z. A., and Yang, Z. M. (2006). Global analysis of differential luminal epithelial gene expression at mouse implantation sites. *J. Mol. Endocrinol.* **37**, 147–161. doi:10.1677/JME.1.02009

Cross, J. C., Werb, Z., and Fisher, S. J. (1994). Implantation and the placenta: key pieces of the development puzzle. *Science* **266**, 1508–1518. doi:10.1126/SCIENCE.7985020

Davies, M. C., Anderson, M. C., Mason, B. A., and Jacobs, H. S. (1990). Oocyte donation: the role of endometrial receptivity. *Hum. Reprod.* **5**, 862–869.

Dawson, P. A., Pirlo, K. J., Steane, S. E., Nguyen, K. A., Kunzelmann, K., Chien, Y. J., and Markovich, D. (2005). The rat Na^+–sulfate cotransporter rNaS2: functional characterization, tissue distribution, and gene (*slc13a4*) structure. *Pflügers Arch.* **450**, 262–268. doi:10.1007/S00424-005-1414-6

Dawson, P. A., Rakoczy, J., and Simmons, D. G. (2012). Placental, renal, and ileal sulfate transporter gene expression in mouse gestation. *Biol. Reprod.* **87**, 43. doi:10.1095/BIOLREPROD.111.098749

Dennis, G., Jr, Sherman, B. T., Hosack, D. A., Yang, J., Gao, W., Lane, H. C., and Lempicki, R. A. (2003). DAVID: Database for Annotation, Visualization, and Integrated Discovery. *Genome Biol.* **4**, P3. doi:10.1186/GB-2003-4-5-P3

Ferretti, C., Bruni, L., Dangles-Marie, V., Pecking, A. P., and Bellet, D. (2007). Molecular circuits shared by placental and cancer cells, and their implications in the proliferative, invasive and migratory capacities of trophoblasts. *Hum. Reprod. Update* **13**, 121–141. doi:10.1093/HUMUPD/DML048

Fluhr, H., Bischof-Islami, D., Krenzer, S., Licht, P., Bischof, P., and Zygmunt, M. (2008). Human chorionic gonadotropin stimulates matrix metalloproteinases-2 and -9 in cytotrophoblastic cells and decreases tissue inhibitor of metalloproteinases-1, -2, and -3 in decidualized endometrial stromal cells. *Fertil. Steril.* **90**(Suppl.), 1390–1395. doi:10.1016/J.FERTNSTERT.2007.08.023

Franco, H. L., Dai, D., Lee, K. Y., Rubel, C. A., Roop, D., Boerboom, D., Jeong, J. W., Lydon, J. P., Bagchi, I. C., Bagchi, M. K., and DeMayo, F. J. (2011). WNT4 is a key regulator of normal postnatal uterine development and progesterone signaling during embryo implantation and decidualization in the mouse. *FASEB J.* **25**, 1176–1187. doi:10.1096/FJ.10-175349

Giritharan, G., Li, M. W., De Sebastiano, F., Esteban, F. J., Horcajadas, J. A., Lloyd, K. C., Donjacour, A., Maltepe, E., and Rinaudo, P. F. (2010). Effect of ICSI on gene expression and development of mouse preimplantation embryos. *Hum. Reprod.* **25**, 3012–3024. doi:10.1093/HUMREP/DEQ266

Giritharan, G., Delle Piane, L., Donjacour, A., Esteban, F. J., Horcajadas, J. A., Maltepe, E., and Rinaudo, P. (2012). *In vitro* culture of mouse embryos reduces differential gene expression between inner cell mass and trophectoderm. *Reprod. Sci.* **19**, 243–252. doi:10.1177/1933719111428522

Gu, X. L., Ou, Z. L., Lin, F. J., Yang, X. L., Luo, J. M., Shen, Z. Z., and Shao, Z. M. (2012). Expression of CXCL14 and its anticancer role in breast cancer. *Breast Cancer Res. Treat.* **135**, 725–735. doi:10.1007/S10549-012-2206-2

Hess, A. P., Hamilton, A. E., Talbi, S., Dosiou, C., Nyegaard, M., Nayak, N., Genbecev-Krtolica, O., Mavrogianis, P., Ferrer, K., Kruessel, J., Fazleabas, A. T., Fisher, S. J., and Giudice, L. C. (2007). Decidual stromal cell response to paracrine signals from the trophoblast: amplification of immune and angiogenic modulators. *Biol. Reprod.* **76**, 102–117. doi:10.1095/BIOLREPROD.106.054791

Hochepied, T., Ameloot, P., Brouckaert, P., Van Leuven, F., and Libert, C. (2000). Differential response of a(2)-macroglobulin-deficient mice in models of lethal TNF-induced inflammation. *Eur. Cytokine Netw.* **11**, 597–601.

Horcajadas, J. A., Pellicer, A., and Simon, C. (2007). Wide genomic analysis of human endometrial receptivity: new times, new opportunities. *Hum. Reprod. Update* **13**, 77–86. doi:10.1093/HUMUPD/DML046

Horcajadas, J. A., Goyri, E., Higon, M. A., Martinez-Conejero, J. A., Gambadauro, P., Garcia, G., Meseguer, M., Simon, C., and Pellicer, A. (2008). Endometrial receptivity and implantation are not affected by the presence of uterine intramural leiomyomas: a clinical and functional genomics analysis. *J. Clin. Endocrinol. Metab.* **93**, 3490–3498. doi:10.1210/JC.2008-0565

Hou, X., Tan, Y., Li, M., Dey, S. K., and Das, S. K. (2004). Canonical Wnt signaling is critical to estrogen-mediated uterine growth. *Mol. Endocrinol.* **18**, 3035–3049. doi:10.1210/ME.2004-0259

Ishida, M., Ohashi, S., Kizaki, Y., Naito, J., Horiguchi, K., and Harigaya, T. (2007). Expression profiling of mouse placental lactogen II and its correlative genes using a cDNA microarray analysis in the developmental mouse placenta. *J. Reprod. Dev.* **53**, 69–76. doi:10.1262/JRD.18002

Jabbour, H. N., Kelly, R. W., Fraser, H. M., and Critchley, H. O. (2006). Endocrine regulation of menstruation. *Endocr. Rev.* **27**, 17–46. doi:10.1210/ER.2004-0021

Johnson, P. M., Christmas, S. E., and Vince, G. S. (1999). Immunological aspects of implantation and implantation failure. *Hum. Reprod.* **14**(Suppl. 2), 26–36. doi:10.1093/HUMREP/14.SUPPL_2.26

Kuang, H., Chen, Q., Zhang, Y., Zhang, L., Peng, H., Ning, L., Cao, Y., and Duan, E. (2009). The cytokine gene *CXCL14* restricts human trophoblast cell invasion by suppressing gelatinase activity. *Endocrinology* **150**, 5596–5605. doi:10.1210/EN.2009-0570

Lea, R. G., and Sandra, O. (2007). Immunoendocrine aspects of endometrial function and implantation. *Reproduction* **134**, 389–404. doi:10.1530/REP-07-0167

Li, Q., Kannan, A., Wang, W., Demayo, F. J., Taylor, R. N., Bagchi, M. K., and Bagchi, I. C. (2007). Bone morphogenetic protein 2 functions via a conserved signaling pathway involving Wnt4 to regulate uterine decidualization in the mouse and the human. *J. Biol. Chem.* **282**, 31 725–31 732. doi:10.1074/JBC.M704723200

Lobo, S. C., Huang, S. T., Germeyer, A., Dosiou, C., Vo, K. C., Tulac, S., Nayak, N. R., and Giudice, L. C. (2004). The immune environment in human endometrium during the window of implantation. *Am. J. Reprod. Immunol.* **52**, 244–251. doi:10.1111/J.1600-0897.2004.00217.X

Marchand, M., Horcajadas, J. A., Esteban, F. J., McElroy, S. L., Fisher, S. J., and Giudice, L. C. (2011). Transcriptomic signature of trophoblast differentiation in a human embryonic stem cell model. *Biol. Reprod.* **84**, 1258–1271. doi:10.1095/BIOLREPROD.110.086413

Masson, V., de la Ballina, L. R., Munaut, C., Wielockx, B., Jost, M., Maillard, C., Blacher, S., Bajou, K., Itoh, T., Itohara, S., Werb, Z., Libert, C., Foidart, J. M., and Noel, A. (2005). Contribution of host MMP-2 and MMP-9 to promote tumor vascularization and invasion of malignant keratinocytes. *FASEB J.* **19**, 234–236.

Meekins, J. W., McLaughlin, P. J., West, D. C., McFadyen, I. R., and Johnson, P. M. (1994). Endothelial cell activation by tumour necrosis factor-alpha (TNF-alpha) and the development of pre-eclampsia. *Clin. Exp. Immunol.* **98**, 110–114. doi:10.1111/J.1365-2249.1994.TB06615.X

Moreno, E. (2008). Is cell competition relevant to cancer? *Nat. Rev. Cancer* **8**, 141–147. doi:10.1038/NRC2252

Murray, M. J., and Lessey, B. A. (1999). Embryo implantation and tumor metastasis: common pathways of invasion and angiogenesis. *Semin. Reprod. Endocrinol.* **17**, 275–290. doi:10.1055/S-2007-1016235

Popovici, R. M., Betzler, N. K., Krause, M. S., Luo, M., Jauckus, J., Germeyer, A., Bloethner, S., Schlotterer, A., Kumar, R., Strowitzki, T., and von Wolff, M. (2006). Gene expression profiling of human endometrial–trophoblast interaction in a coculture model. *Endocrinology* **147**, 5662–5675. doi:10.1210/EN.2006-0916

Rakoczy, J., Dawson, P., and Simmons, D. (2014). Loss of placental sulphate transporter Slc13a4 causes severe developmental defects and embryonic lethality. *Placenta* **35**, A96–A97. doi:10.1016/J.PLACENTA.2014.06.313

Ren, L., Liu, Y. Q., Zhou, W. H., and Zhang, Y. Z. (2012). Trophoblast-derived chemokine CXCL12 promotes CXCR4 expression and invasion of human first-trimester decidual stromal cells. *Hum. Reprod.* **27**, 366–374. doi:10.1093/HUMREP/DER395

Shea, K., and Geijsen, N. (2007). Dissection of 6.5 dpc mouse embryos. *J. Vis. Exp.* **2**, e160.

Smith, S. K. (2000). Angiogenesis and implantation. *Hum. Reprod.* **15**(Suppl. 6), 59–66.

Stuckenholz, C., Lu, L., Thakur, P. C., Choi, T. Y., Shin, D., and Bahary, N. (2013). Sfrp5 modulates both Wnt and BMP signaling and regulates gastrointestinal organogensis in the zebrafish, *Danio rerio*. *PLoS ONE* **8**, e62470. doi:10.1371/JOURNAL.PONE.0062470

Su, H. Y., Lai, H. C., Lin, Y. W., Liu, C. Y., Chen, C. K., Chou, Y. C., Lin, S. P., Lin, W. C., Lee, H. Y., and Yu, M. H. (2010). Epigenetic silencing of SFRP5 is related to malignant phenotype and chemoresistance of ovarian cancer through Wnt signaling pathway. *Int. J. Cancer* **127**, 555–567. doi:10.1002/IJC.25083

Takagi, H., Sasaki, S., Suzuki, H., Toyota, M., Maruyama, R., Nojima, M., Yamamoto, H., Omata, M., Tokino, T., Imai, K., and Shinomura, Y. (2008). Frequent epigenetic inactivation of SFRP genes in hepatocellular carcinoma. *J. Gastroenterol.* **43**, 378–389. doi:10.1007/S00535-008-2170-0

The R Development Core Team (2004). 'R: A Language and Environment for Statistical Computing.' (R Foundation for Statistical Computing: Vienna.)

Tulppala, M., Julkunen, M., Tiitinen, A., Stenman, U. H., and Seppala, M. (1995). Habitual abortion is accompanied by low serum levels of placental protein 14 in the luteal phase of the fertile cycle. *Fertil. Steril.* **63**, 792–795.

van der Horst, P. H., Wang, Y., Vandenput, I., Kuhne, L. C., Ewing, P. C., van Ijcken, W. F., van der Zee, M., Amant, F., Burger, C. W., and Blok, L. J. (2012). Progesterone inhibits epithelial-to-mesenchymal transition in endometrial cancer. *PLoS ONE* **7**, e30840. doi:10.1371/JOURNAL.PONE.0030840

Yoshinaga, K. (2008). Review of factors essential for blastocyst implantation for their modulating effects on the maternal immune system. *Semin. Cell Dev. Biol.* **19**, 161–169. doi:10.1016/J.SEMCDB.2007.10.006

Zhou, Y., Damsky, C. H., and Fisher, S. J. (1997). Preeclampsia is associated with failure of human cytotrophoblasts to mimic a vascular adhesion phenotype. One cause of defective endovascular invasion in this syndrome? *J. Clin. Invest.* **99**, 2152–2164. doi:10.1172/JCI119388